Hydrogen Bond Surface Chemistry: Interaction of NH_3 with an Ice Particle

Nevin Uras[†]

The Fritz Haber Institute for Molecular Dynamics, Hebrew University, Jerusalem, 91904, Israel and Department of Chemistry, Oklahoma State University, Stillwater, Oklahoma 74078

Victoria Buch*[,‡]

The Fritz Haber Institute for Molecular Dynamics, Hebrew University, Jerusalem, 91904, Israel

J. Paul Devlin[§]

Department of Chemistry, Oklahoma State University, Stillwater, Oklahoma 74078

Received: May 8, 2000; In Final Form: July 25, 2000

The study focuses on interaction of a "strong" adsorbate with an ice surface. Ammonia adsorption on an ice cluster $(H_2O)_{293}$ is investigated by Monte Carlo simulations, as a function of coverage at $T = 110$ K. At low coverages, ammonia is attached to dangling H-atoms on the surface, while forming additional weaker bonds with neighboring dangling O. At high coverages insertion is observed of the NH_3 molecules into the surface. The process is driven by the ability of NH_3 molecules to cleave strained $H_2O\cdots H_2O$ hydrogen bonds in the ice surface, and to form strong $N\cdots HO$ bonds with the water molecules.

I. Introduction

Water ice is an interesting and a basic solid. Its molecular properties are determined by the unique ability of the H_2O molecule to form four relatively strong hydrogen bonds to four neighboring water molecules, in an approximately tetrahedral arrangement.[1,2] Gas adsorption on icy surfaces is of interest in terrestrial, atmospheric and interstellar chemistry.[3] While numerous studies have been carried out in the past in these contexts on ice−adsorbate systems, molecular level investigations of ice−adsorbate interactions (at a solid−vacuum interface) are a relatively new topic. Examples of recent work by other authors on ice−adsorbate systems include second harmonic generation[4] and infrared spectroscopy,[6−8] He scattering,[5] and adsorbate photodissociation studies.[9] Theoretical modeling has been also pursued in connection with the atmospherically relevant HCl−ice interaction,[10−12] and for a number of other ice−adsorbate systems as well (e.g. refs 7 and 13). A related experimental−theoretical work has been carried out on NH_3 adsorption at the air−liquid water interface.[14] There is considerable similarity in bonding configurations found in this study for ammonia on ice, and the ones proposed for the liquid.

The present study is a continuation of a series of joint theoretical-experimental investigations, aiming at molecular level understanding of icy surfaces, and of ice adsorbate−interactions.[15] In the past, detailed theoretical−experimental studies were directed at adsorbates such as H_2[16] and CF_4,[17] whose bond strength to H_2O is significantly smaller than the $H_2O\cdots H_2O$ hydrogen bond. These adsorbates adapt themselves to the ice surface structure, occupying sites such as centers of water rings, and being attached to the surface by multiple weak interactions with numerous H_2O. Recently, a series of experimental investigations was carried out of the interaction of ice nanocrystals with more "active" adsorbates, characterized by a larger bond strength to H_2O; these adsorbates are attached to the surface while modifying the ice hydrogen bond network.[18−20] Beyond monolayer coverage, molecules that form strong H-bonds with H_2O, such as ammonia, HCl, and ethylene oxide were shown to proceed to penetrate into ice, forming a mixed hydrate solid.[19,20] The conversion is characteristic of adsorbates capable of forming stronger bonds with H_2O than with each other. The penetration process is driven by the energy gain from formation of the hydrate, with respect to formation of multiple adsorbate layers. Interestingly, both strong Lewis bases and strong acids follow the above pattern. Diverse types of solids can be formed in this process:[19] Ethylene oxide converts ice to type I clathrate hydrate. HCl, which at low coverage is adsorbed in a surface layer,[20] ionizes while forming a hydrate. Ammonia forms a monohydrate or a hemihydrate via a molecular mechanism.

The first steps of this "hydrogen bond chemistry" are simulated in the present study, for the NH_3 adsorbate. Adsorbate interaction is studied with a 2.6 nm ice particle. Monte Carlo (MC) simulations are used to calculate the structure of the ice−adsorbate system, as a function of coverage. Initial stages of adsorbate penetration into ice are reproduced and analyzed in terms of intermolecular interactions, and the hydrogen bond network rearrangement.

Section II is a brief summary of the pertinent experimental results. In section III details of the simulation are given. In section IV results of the simulations are presented. A summary is given in section V.

II. Summary of Pertinent Experimental Results

NH_3 adsorption on D_2O ice nanocrystals was investigated by infrared spectroscopy; details can be found in ref 19. The ammonia molecule forms a strong hydrogen bond with H_2O as a proton acceptor, in the $OH\cdots N$ configuration; on the other

[†] E-mail: nevin@okstate.edu.
[‡] E-mail: viki@fh.huji.ac.il.
[§] E-mail: devlin@okstate.edu.

10.1021/jp0017240 CCC: $19.00
Published on Web 09/13/2000

hand, it is a notoriously weak proton donor. Initial exposure of ice to NH_3 at submonolayer coverages is associated with adsorbate bonding to dangling OD, as evidenced by disappearance of the bare dangling OD band at 2725 cm^{-1}. Near complete monolayer coverage, the dangling OD red shift attained the maximal value of about 500 cm^{-1}, far above that induced by weak adsorbates. The shifted dangling OD band (at $\sim$ 2200 cm^{-1}) is even to the red from the hydrogen-bonded OD band of ice (peaking at 2400 cm^{-1}), suggesting that the OD$\cdots$N hydrogen bond is stronger than that between water molecules in ice. An array of D_2O nanocrystals, exposed to $\sim$2 μm pressure of NH_3 (g) at 120 K, is converted to a hydrate solid over a period of hours. Initially, the product is the amorphous hydrate of ammonia, but after 20% conversion, crystalline monohydrate becomes a dominant product. During the experiment, no conversion of D_2O to HDO was observed, which shows that the hydrate formation mechanism is molecular rather than ionic. In addition to studies of NH_3(g) adsorption from the gas phase,[19] some preliminary spectroscopic studies were carried out of interpenetration of D_2O and NH_3 films in contact; the product was ammonia hemihydrate rather than monohydrate.

III. Simulations

A. Ice Particle Model. At low temperatures ice particles tend to freeze into a cubic ice form (ice Ic[1,2,21,22]). In a perfect cubic ice crystal O-atoms form a periodic pattern which can be viewed as stacked puckered hexagonal bilayers.[1,2] Each O-atom has four nearest-neighbor O-atoms in a tetrahedral arrangement; between each near neighbor O pair there is an H-atom which is chemically bonded to one of the O-atoms, and hydrogen bonded to another. Thus, an H-atom can occupy one of the two possible sites. There is a large number of H-atom arrangements which are allowed according to the so-called "ice rules", which state that each O-atom is chemically bonded to two H-atoms forming an intact water molecule, and hydrogen bonded to two additional H-atoms chemically bound to neighbors.[1,2] Thus, ice Ic is "proton-disordered" (or, more precisely, orientationally disordered). The common hexagonal ice Ih is very similar, differing only in the stacking order of the hexagonal bilayers.[1,2]

Molecular structure of ice particles was investigated by Torchet et al.[21] and Bartell et al.[22] using electron diffraction, and by ourselves using a combination of infrared spectroscopy and computational modeling.[17,18,23] Cubic ice diffraction patterns were obtained for clusters containing thousands of water molecules;[21,22] however the clusters were shown to include a disordered component. Our studies suggest that ice clusters and nanocrystals are characterized by a crystalline core and a disordered surface;[17,23] the two components are connected by strained but mostly crystalline "subsurface". This is since an approximately spherical shape, while ensuring small surface area, is not compatible with crystalline surface structure. Spectroscopic signature of the (strained) crystalline component persists down to the cluster size of several hundred molecules, and disappears near mean cluster diameter of $\sim$2 nm ($\sim$120 water molecules).

The simulations were carried out on an $(H_2O)_{293}$ particle. The experiments were with particles of diameter 50 nm, with millions of water molecules. However since there is evidence for disordered surface structure in both small and large particles,[17,23] we believe that considerable insight can be gained from the small model. (There is, however, spectroscopic evidence for some difference in the surface texture of small and large particles; e.g., in the latter, the percentage of dangling atoms seems to be larger.[23])

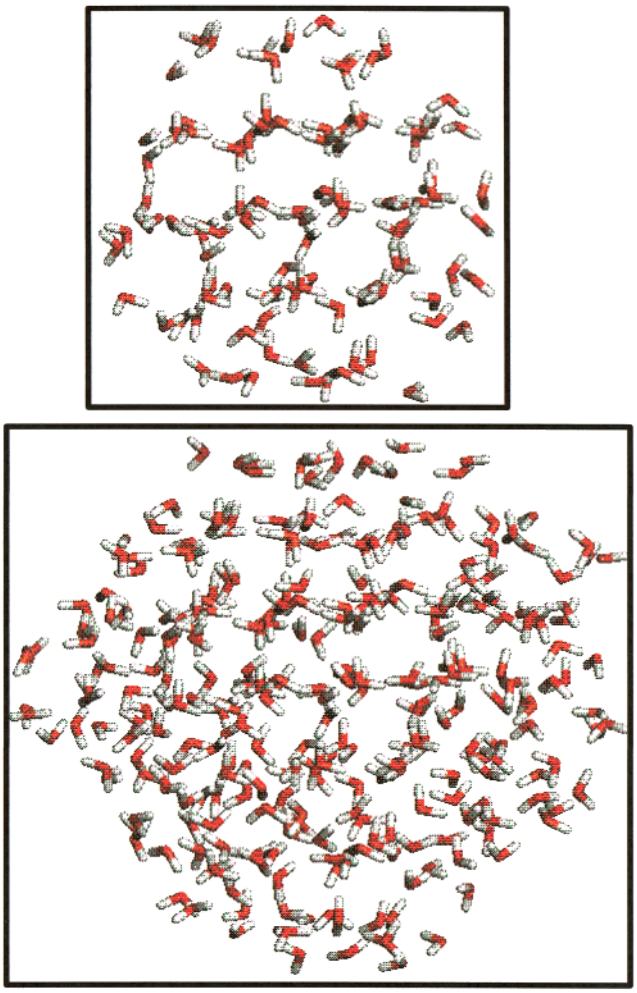

Figure 1. Bottom: snapshot of the 2.6 nm ice particle $(H_2O)_{293}$ from the 110 K simulation at low ammonia coverage (NH_3 is not shown). Top: the particle core; 104 interior molecules within diameter of 1.8 nm are shown. The remains of crystalline order are apparent in the core.

The model was constructed similarly to ref 23. First, a proton disordered idealized cubic ice structure was constructed using a method of ref 24. Molecules within a sphere of diameter 2.6 nm were included in the model. This procedure generates a crystalline particle with numerous "broken bonds" and high energy molecules at the surface. The following empirical procedure was used to relax the surface:[23] (a) the model was heated by molecular dynamics to 180 K, (b) a classical trajectory was run for 45 ps, and (c) the final structure was recooled to 70 K and minimized. TIP4P potential was employed in these calculations.[25]

The latter minimized structure was used in simulations employing a rigid surface model and, as input, in more realistic simulations, in which both water and ammonia molecules were subjected to Monte Carlo steps. Figure 1 shows a snapshot of cluster structure from a 110 K simulation at low ammonia coverage. While considerable molecular disorder is apparent, the cluster core, shown in the upper panel, retains to a significant extent the initial crystalline structure.

B. Potential. In this initial study, nonpolarizable potential surface (PES) was employed. The monomers were assumed rigid. (As noted above, there is experimental evidence that NH_3 molecules remain intact after adsorption on ice.) TIP4P potential was used for water$-$water interactions.[25] For NH_3 $-NH_3$

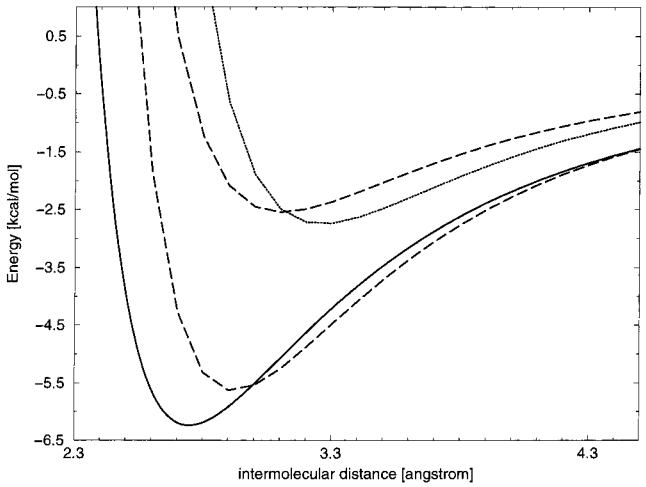

Figure 2. Intermolecular interactions. Solid: TIP4P OH···O water−water interaction. Dashed, bottom: water−ammonia interaction, in the OH···N bonding configuration. Dashed, top: water−ammonia interaction, in the O···HN configuration. Dotted: NH_3···NH_3 interaction, in NH···N-bonded configuration.

interaction, the potential of ref 26 was adopted. Monomer geometries were adopted from the respective two potentials.[25,26]

The NH_3···H_2O potential was constructed by fitting to an ab initio study of Rzepkowska and Sadlej.[27,28] In that study, the PES was mapped out using MP2 level supermolecular method, with aug-cc-pVTZ Dunning basis,[29] and counterpoise correction of Boys and Bernardi.[30] The fitted nonpolarizable potential included 3 point charges on H_2O, four point charges on NH_3, and a Lennard-Jones interaction $4\epsilon[(\sigma/r)^{12} - (\sigma/r)^6]$ centered at O- and N-atoms; $\epsilon = 0.2076$ kcal/mol; $\sigma = 3.27$ Å. The positive charges were placed on H-atoms, $q = 0.62$e for H_2O, and $q = 0.462$e for NH_3. The negative charges were placed on the H_2O bisector, and on the ammonia C_3 axis, 0.2677 and 0.156 Å from O and N toward the H-atoms, respectively. In the negative PES region, the standard deviation between the fit and 41 ab initio points was 0.33 kcal/mol. The rotational constants of the NH_3···H_2O dimer calculated with this PES (using DMC[31]) are 152667, 6150, and 6095 MHz as compared to the experimental values[32] of 147714, 6169, and 6111 MHz (the last two constants match the experiment within DMC accuracy, which is a few tens of megahertz; the first is hard to calculate accurately using DMC[31]). More details on the NH_3···H_2O potential will be given in a separate publication.[28,33]

Figure 2 shows the H_2O···NH_3, NH_3···NH_3 and H_2O···H_2O interaction for potentials used, for favorable mutual orientations. It is seen that the binding energy of H_2O···NH_3 for the ammonia proton acceptor configuration is 5.6 kcal/mol, while the ammonia proton donor configuration is bound much more weakly. The binding energy for NH_3···NH_3 is similar to that of H_2O···NH_3 in the O-bonded configuration. The TIP4P H_2O···H_2O binding energy is 6.2 kcal/mol. One may note at this point that the NH_3···NH_3 and H_2O···H_2O interactions were calibrated against condensed phases, while H_2O···NH_3, against the isolated dimer data. In condensed phases, polarizability is expected to increase the bond strength with respect to isolated dimer. Thus, H_2O···NH_3 interaction is underestimated in this study.

Cutoff of 13 Å for intermolecular interactions was used to calculate the system energy. A shorter cutoff of 9 Å was used to calculate energy change during MC steps.

C. Monte Carlo Simulation. A canonical MC simulation was used, at $T = 110$ K. (The temperature value was selected from within the range of pertinent experimental studies, 100−120 K.) A fixed number of NH_3 molecules was initially deposited at random on the cluster surface. Simulation was run until system properties appeared to stabilize, on the average. An MC step included a rotation and a translation of a randomly selected molecule. The translational steps were chosen from the Gaussian distribution, with $\sigma = 0.045$ and 0.06 Å for water and ammonia, respectively. Rotation vectors υ_r were also selected from a Gaussian distribution, with $\sigma = 2°$ for both molecules. Rotations were carried out around υ_r according to formulas given in ref 34. The length of each simulation was about 6×10^7 MC trial steps. Most of the analysis given below is based on final configurations at coverages of 16, 76, and 143 NH_3 molecules.

To elucidate the influence of H_2O relaxation, a simulation at each coverage was also run for the case in which H_2O molecules were frozen at the cluster minimum configuration (results denoted "fr" in Table 1). The moving water ("mw") simulations were initiated using the frozen water results as input.

TABLE 1: NH_3 and H_2O Coordination[a]

property no. of NH_3	16(fr)	16(mw)	76(fr)	76(mw)	143(fr)	143(mw)
			Total Number of H-Bonds[b]			
OH···O	552	547	552	505	552	482
OH···N	15	15	31	73	34	99
NH···O	5	19	53	116	88	171
NH···N	1	2	57	25	189	119
			Water Coordination[c,d]			
H2O3	6	11	6	4	6	2
H2O2	220	202	220	173	220	161
H2O1	33	42	33	50	33	47
H1O2	27	29	27	24	27	26
H1O1	7	6	7	21	7	23
H0O2		2		9		9
H2O0		1		2		4
H0O1				7		11
H1O0				2		4
H0O0						5
total d−H	34	39	34	81	34	104
total d−O	40	49	40	82	40	94
			NH_3 Coordincation[d,e]			
s2w4						2
s2w3				1		1
s2w2				3		5
s1w5			5			1
s1w4				3	2	6
s1w3		1	1	9	2	13
s1w2	1	3	5	26	9	33
s1w1	3	8	20	21	13	26
s1w0	11	3		4	8	4
s0w6					2	
s0w5			2	2	7	6
s0w4			7		24	11
s0w3			14	3	47	17
s0w2	1	2	18	3	23	17
s0w1			4		5	1

[a] mw denotes a simulation with moving water. Simulation with H_2O configuration frozen at a cluster minimum is denoted fr. [b] H-bonds are determined using an H···N or H···O cutoff distance. Cutoffs of 2.3, 2.4, 2.6, and 2.8 Å were used for OH···O, OH···N, NH···O and NH···N, respectively. [c] notation such as H1O2 means "one bond through H, two bonds through O". The table shows the number of H_2O in a given configuration obtained in the simulation. [d] rare coordinations which appear only once were not included. [e] notation such as s1w2 means "one strong bond, two weak bonds". A strong bond is OH···N. Weak bonds are NH···N and NH···O. The table shows the number of NH_3 in a given configuration obtained in the simulation.

IV. Results

The results are shown in Figures 3−6, and in Table 1. Table 1 presents numbers of hydrogen bonds of various kinds. To

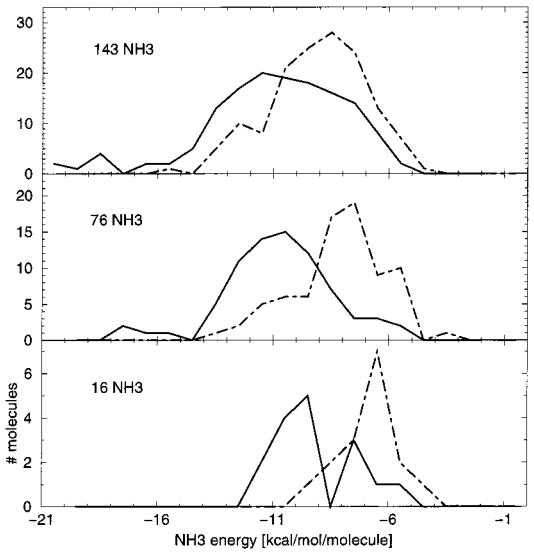

Figure 3. Distribution of NH_3 energies. NH_3 energy was taken as a sum of all its interactions with water and other NH_3 within a 13 Å cutoff. Solid: moving water simulation. Dot−dashed: frozen water simulation. Coverages are indicated in the respective panels.

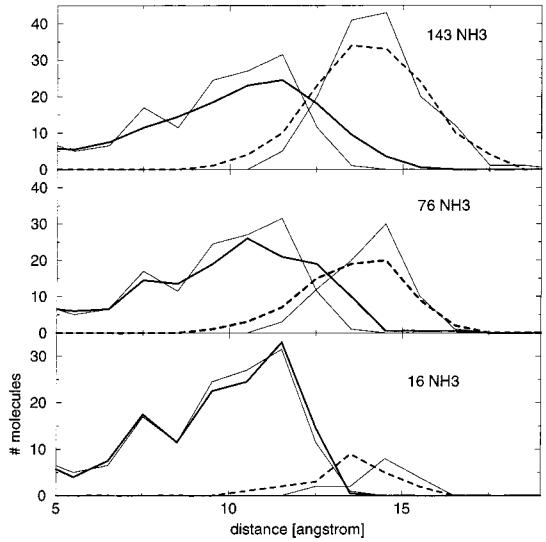

Figure 4. Distribution of molecular distances from the cluster center of mass. Coverages are indicated in the respective panels. Thick solid line, water and, dashed, ammonia in the simulation with moving water. Left and right thin solid line pertains to water and ammonia, respectively, in fw simulation in which H_2O was not allowed to move. The water distributions were multiplied by 0.5.

determine the number of hydrogen bonds, distributions of O···H and N···H distances were first calculated for the highest coverage examined. The cutoff distances for hydrogen bonding were determined as the first minima in the O···H or N···H distribution functions for H_2O-H_2O, H_2O-NH_3 and NH_3-NH_3 pairs; see the table footnote for cutoff values.

A. Glossary. (a) d-H: a dangling H-atom of H_2O, that is, an H-atom which does not have an O-neighbor within 2.3 Å. (b) d-O, a dangling O-atom, denotes an atom which has one or zero H-neighbors belonging to other water molecules within 2.3 Å. In the course of the simulation d-H- and d-O-atoms form bonds to NH_3. *It is emphasized that an atom is denoted below as "dangling" irrespective of whether it is bonded to adsorbate.* (c) "fr" simulations: simulations in which H_2O are frozen at bare cluster minimum positions. (d) In "mw" simulations both water and adsorbate were subjected to Monte Carlo steps. (e) Notation such as H2O1 describes coordination of an H_2O molecule with respect to other water molecules. It means "two hydrogen bonds through H, and one hydrogen bond through O". (f) Notation such as s1w2 describes coordination of NH_3 with respect to either water or other NH_3 molecules. "s1" means "one strong N···HO bond to water"; "w2" means "two additional weak bonds, either to water oxygen, or to another ammonia"; the two kinds of weak bonds correspond to similar bond strengths.

B. General Features of Physical Behavior. Dangling H-atoms of H_2O provide easily accessible strong binding sites for NH_3 on the cluster surface. The ammonia bonding to d-O is weaker by about a factor of 2. At the cluster minimum, there are 34 d-H and 40 d-O on the bare cluster surface. These numbers fluctuate; during a 110 K simulation of the cluster we may have several more dangling atoms solely due to thermal fluctuations. (I. e., a thermal fluctuation may cause a slight increase in an intermolecular distance, beyond the 2.3 Å cutoff value for hydrogen bonding.) At low coverage, NH_3 molecules are attached to the available binding sites on the surface. When the number of adsorbate molecules exceeds the number of d-H sites, ammonia actively generates new favorable surface sites, by cleaving the $H_2O\cdots H_2O$ bonds. Thus, NH_3 adsorbate rearranges the surface structure. More details are given below.

C. Low Coverage (16 NH_3). At 16 NH_3 coverage, the number of adsorbate molecules is a factor of 2 smaller than the number of available d-H sites on the cluster surface. Nearly all adsorbate molecules become in fact connected to d-H in the course of both the frozen water and the moving water simulations (see Table I and Figure 5A). Nevertheless, it is seen in Figure 3 that water relaxation contributes significantly to ammonia bonding; that is, NH_3 energy distribution for mw peaks at values more negative by some 50% than for fw. This is since in mw, most of NH_3 acquire, in addition to strong OH···N bonds, weak bonds to O-atoms of water, in the NH···O configuration. *Thus, NH···O bonds constitute a substantial contribution to the binding energy, in addition to the stronger OH···N bonds.* It is seen in Figures 4 and 5A that NH_3, which are protruding from the surface in fw, assume more "sunken" positions on the surface in mw. H_2O molecules with dangling H-atoms rotate to allow for this additional bonding. Moreover the adsorbate seems to be able to change the location of d-O-atoms; three of the "new" NH···O bonds obtained in mw are to d-O molecules such that the O-atom was fully coordinated in the frozen model. (See new NH···O bonding of the ammonia molecule in the middle-left part of the cluster in Figure 5A.) Also, in the course of the mw simulation some NH_3 molecules move to a new d-H site.

D. Intermediate Coverage (76 NH_3). At this coverage, the number of NH_3 molecules exceeds by a factor of 2 the number of the d-H sites originally available on the cluster surface. In this case, the effect of surface reconstruction is large and visually apparent (see Figures 5B and 6).

In the fw simulation (Figure 5B, top), ammonia molecules cluster on the surface, around the available d-H sites (compare to the low coverage Figure 5A, top). In addition to 31 strong OH···N bonds (whose number is close to the number of d-H-atoms), there are 110 weak bonds, half to O-atoms of water, and half between adsorbate molecules. However when water molecules are allowed to move, nearly all ammonia molecules manage to acquire a strong OH···N bond (see Table 1). In the process, 47 $H_2O\cdots H_2O$ bonds are cleaved. In addition to new strong bonds, ammonia insertion into the surface is associated with formation of numerous new weak NH···O bonds. The latter

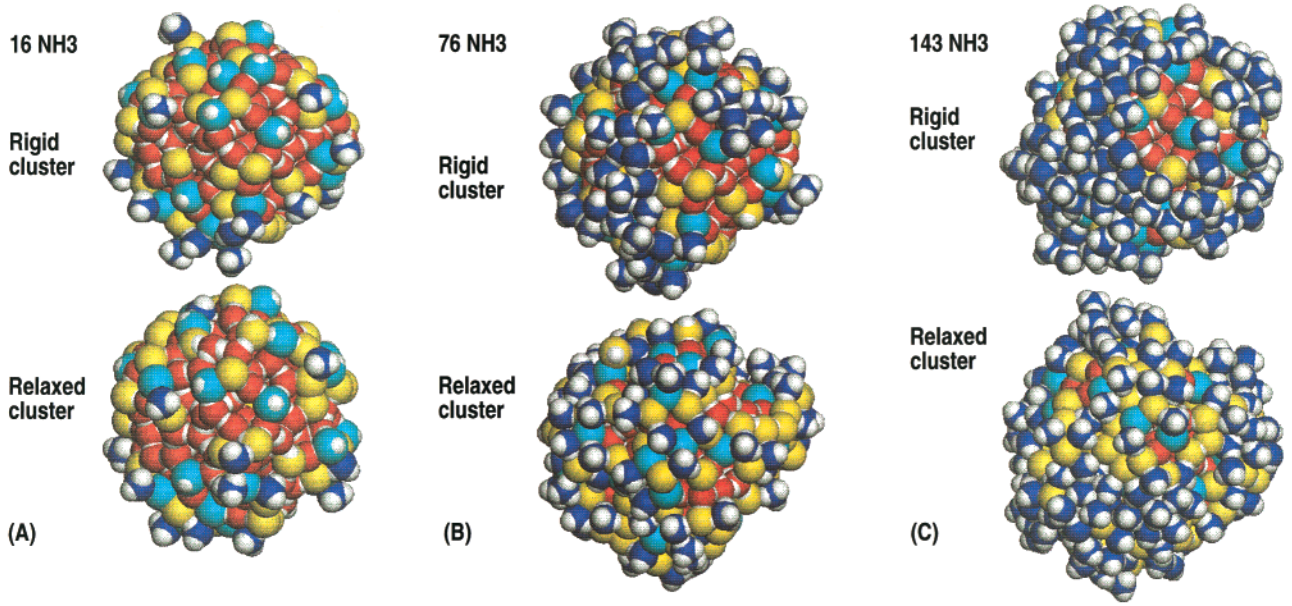

Figure 5. Snapshots of a cluster covered by NH_3 at 110 K, at coverages of 16 NH_3 (A), 76 NH_3 (B), and 143 NH_3 (C). The top figure corresponds to fw simulation in which H_2O molecules were not allowed to move. N-atoms are marked dark blue. O-atoms of "dangling H_2O" are marked yellow or light blue. "Dangling H_2O" is defined as a molecule with coordination lower than 4 with respect to other water molecules. Light blue denotes H_2O with dangling H-atom(s) and saturated O coordination. Yellow denotes H_2O with a dangling O-atom (and, possibly, a dangling H). O-atoms of H_2O fully coordinated with respect to other water molecules are marked red.

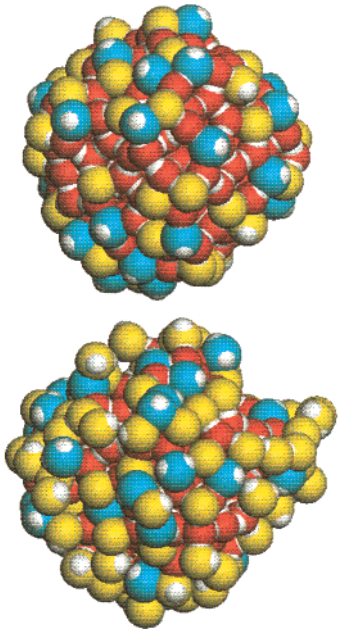

Figure 6. Water cluster, with ammonia molecules removed. Notation as in Figure 5. Bottom: snapshot from the 76 NH_3 simulation (corresponds to Figure 5B). Top: cluster minimum, used in the fw simulations. The figure shows increase in "dangling H_2O" concentration on the cluster surface, as a result of interaction with asdorbate.

happens at the expense of significant reduction in the number of the second kind of weak bonds, $NH_3\cdots NH_3$, which are of comparable strength. As seen in Figure 5B (bottom), dense clumps of NH_3 molecules disappear from the surface. Instead, NH_3 forms segments of chainlike structures, flanked by water molecules with dangling atoms (dangling with respect to water, but participating in bonding to adsorbate).

Figure 6 (bottom) shows the water cluster configuration, with 76 adsorbate molecules removed. Marked in blue and yellow are water molecules with dangling H- or O-atoms (dangling with respect to other water molecules, but largely connected to ammonia). The figure shows a significant increase in the number of dangling water atoms on the surface, with respect to the "rigid cluster" model, and a protrusion on the right side, generated by interaction with the adsorbate. Change in cluster shape induced by adsorbate is an interesting phenomenon to be investigated in the future.

E. High Coverage (143 NH_3). In the mw calculation, additional $H_2O\cdots H_2O$ bonds are destroyed upon increased NH_3 coverage (see Figure 5C). However here adsorbate insertion appears to saturate at 99 strong $OH\cdots N$ bonds. In the experiment, at $T > 100$ K ammonia molecules proceed to penetrate ice particles and to convert them to a hydrate.[19,35] The process, being activated, becomes too slow to monitor experimentally below 90 K. Under present simulation conditions further penetration does not occur. It is likely that the activation barrier for surface insertion is less than for deeper penetration, since surface $H_2O\cdots H_2O$ bonds are strained. Moreover, as discussed in section II, $NH_3\cdots H_2O$ interaction is most likely underestimated in the present model.

F. Typical Water and Adsorbate Coordination at Intermediate and High Coverage. Initial stages of mutual interpenetration of water and ammonia in mw simulations are evident from Figure 4. We focus first on the changes in water coordination as a result of NH_3 bonding in mw simulations. Comparison of water coordinations to the frozen cluster case (see Table 1) shows reduction in "normal" four coordinated species H2O2, and concurrent significant increase in 3-coordinated d-O molecules (H2O1), and in two coordinated H1O1 molecules. (See glossary above for the notation.) In addition, new water configurations are generated, which are absent in the bare cluster, and, more generally, unusual for bare ice surfaces.[36,37] These configurations are characterized by low coordination (0−2) with respect to other water molecules. In most of the corresponding H_2O molecules both H-atoms of water are dangling; the "new" d-H-atoms are of course connected to ammonia.

While d-H-atoms form single strong bonds to NH_3, a d-O-atom can accept up to 3 weak bonds from NH_3. At high

coverage, most of d-O-atoms form either one or two bonds to NH_3, in addition to a single bond to another H_2O.

The total number of H-bonds formed by NH_3 is in the range 1−5. For most of the ammonia molecules, one bond is strong, and the rest, weak (see Table I).

These results can be related to the ammonia monohydrate and hemihydrate, observed experimentally after completion of NH_3 penetration to ice[19,38] (see section II). Ammonia hemihydrate is a three-dimensional network of alternating nitrogen and oxygen atoms connected by H-bonds of NH···O and OH···N variety, but using only one of the two types of ammonia. The other ammonia makes a single H-bond as a proton acceptor from the water of the network (and dangles into a channel). Overall, the water molecules are five coordinated, donating both protons and accepting three protons each. The ammonia of the network makes four H-bonds. The OH···N distances are all nearly 2.85 Å while the NH···O distances are between 3.13 and 3.22 Å. The structure is nearly tetrahedral about the nitrogens of the network.

Ammonia monohydrate consists of planar chains of water molecules connected by OH···O bonds of length 2.76 Å. These chains are cross-linked by the ammonia molecules via short OH···N bonds (2.775 Å) and long weak NH···O bonds ranging from 3.21 to 3.29 Å. The water is 6-coordinated; each H_2O is a proton acceptor to three NH_3 and one water, and a proton donor to one ammonia and one water. The ammonia molecules are 4-coordinated (three as donor and one as acceptor).

In the mw simulation, we observe initial stages of the approach toward these structures, including reduction of the surface H_2O coordination with respect to other water molecules, and appearance of O-acceptor bonding to more than two molecules. The value obtained for the nearest neighbor peak in the OH···N bond length distribution (in high and medium coverage simulations) is 2.88 Å, similar to the hemihydrate value. The O···HN first nearest neighbor distribution is doubly peaked at 2.98 and 3.09 Å for medium coverage, and 2.99 and 3.14 Å for high coverage; thus the distribution seems to move toward larger hydrate values. The hydrates are characterized by high coordination of O-atoms as proton acceptors (three or four). On the surface, the coordination of d-O-atoms is mostly lower, and somewhat stronger O···HN bonds are consistent with less crowding.

V. Summary

This article addressed Monte Carlo modeling of the interaction between ice, and a "strong" adsorbate, ammonia. Exposure to excess adsorbates, which form strong bonds to H_2O, was shown experimentally to result in adsorbate penetration into the surface, and finally in conversion to mixed hydrate solids.[19,35] First stages of this hydrogen bond chemistry are investigated theoretically for the first time. Atomic level MC simulation focuses on an ice particle $(H_2O)_{293}$, whose surface is exposed to various coverages of NH_3, at $T = 110$ K. The resulting structure of the surface layer of the particle was examined, and initial stages of adsorbate penetration were in fact observed.

Generally, the physical behavior of the system is determined by availability of dangling H-atoms on the particle surface. The d-H-atoms provide strong binding sites for the adsorbate, which is an excellent proton acceptor. At low coverage, sufficient d-H-atoms are available to accommodate all NH_3 molecules. *At high coverages, strong binding sites are actively generated by NH_3 by cleavage of surface H_2O···H_2O bonds*. The cleavage results both in a strong bond of NH_3 to a dangling H-atom of water (N···OH), and one or more weaker bonds to dangling O (NH···O). The process is driven by the fact that N···OH bonds are much stronger than bonding between ammonia molecules, and of comparable strength to OH···O bonds.

The main limitation of this initial study is the use of nonpolarizable potentials. For H_2O···H_2O and NH_3···NH_3, "effective" condensed phase potentials were used, which include the average effect of many-body forces.[25,26] However for H_2O···NH_3, an analytic fit to a dimer ab initio calculation was used. Many body forces are expected to increase the strength of the H_2O···NH_3 interaction. It is remarkable that even this underestimated adsorbate−surface interaction is sufficient to initiate adsorbate insertion into the surface; this is since H_2O···H_2O interactions are significantly reduced with respect to the optimal value by surface strain. Future extension of this work will employ polarizable potentials, which appear necessary for a study of further penetration of NH_3 into the solid surface.

One may note finally a recent related study by Donaldson, focusing on adsorption of NH_3 at the air−liquid water interface; the study included thermodynamic and kinetic analysis of surface tension measurements, in conjunction with ab initio investigations of NH_3···H_2O and NH_3···$(H_2O)_2$ complexes.[14] On the basis of this analysis, NH_3 was proposed to be attached to the liquid surface by one strong N···OH bond, and one or two weaker NH···O bonds. Thus, there appears to be considerable similarity in bonding of NH_3 adsorbate to liquid and solid H_2O surfaces.

Acknowledgment. Support of the Binational Science Foundation, Grant 9800208, and the National Science Foundation, Grant 9617120 is gratefully acknowledged.

References and Notes

(1) Hobbs, P. V. *Ice Physics*; Clarendon: Oxford, U.K., 1974.
(2) Petrenko, V. F.; Whitworth, R. W. *Physics of Ice*; Oxford University Press: Oxford, U.K., 1999.
(3) (a) Molina, M. J.; Tso, T. L.; Molina, L. T.; Wang, F. C. Y. *Science* **1987**, *238*, 1253. (b) McCoustra, M. R. S., and Horn, A. B. *Chem. Soc. Rev.* **1994**, *23*, 195. (c) Tolbert, M. A.; Rossi, M. J.; Malhorta, R.; Golden, D. M.; *Science* **1987**, *238*, 1258. (d) Tielens, A. G. G. M.; Allamandola, L. J. In *Physical Processes in Interstellar Clouds*; Morfill, G. E., Scholet, M., Eds.; Reidel: Dordrecht, 1987. (e) Buch, V. In *Molecular Astrophysics*; Hartquist, W. T., Ed.; Cambridge University: Cambridge, U.K., 1990.
(4) Geiger, F. M.; Tribico, A. C.; Hicks, J. M. *J. Phys. Chem. B.* **1999**, *103*, 8205.
(5) Graham, A. P.; Menzel, A.; Toennies, J. P. *J. Chem. Phys.* **1999**, *111*, 1169.
(6) (a) Horn, A. B.; Chesters, M. A.; McCoustra, M. R. S.; Sodeau, J. R. *J. Chem. Soc., Faraday Trans*. 19992, 88, 1077. (b) Schaff, J. E.; Roberts, J. T. *J. Phys. Chem.* **1996**, *100*, 14151.
(7) Allouche, A.; Verlaque, P.; Pourcin, J. *J. Phys. Chem. B* **1998**, *102*, 89.
(8) Couturier-Tamburelli, I.; Chiavassa, T.; Pourcin, J. *J. Phys. Chem. B* **1999**, *103*, 3677.
(9) Rieley, H.; Colby, D. J.; McMurray, D. P.; Reeman, S. M. *J. Phys. Chem. B* **1997**, *101*, 4982.
(10) Al-Halabi, A.; Kleyn, A. W.; Kroes, G. J. *Chem. Phys. Lett.* **1999**, *307*, 505.
(11) Kroes, G. J.; Clary, D. C. *J. Phys. Chem.* **1992**, *96*, 7079.
(12) Bussolini, G.; Casassa, S.; Pisani, C.; Ugliengo, P. *J. Chem. Phys.* **1998**, *108*, 9516.
(13) Allouche, A. *J. Phys. Chem. A* **1999**, *103*, 9150.
(14) Donaldson, D. J. *J. Phys. Chem. A* **1999**, *103*, 62.
(15) Reviews: Devlin, J. P.; Buch, V. *J. Phys. Chem.* **1995**, *99*, 16534; *J. Phys. Chem. B* **1997**, *101*, 6095.
(16) Buch, V.; Devlin, J. P. *J. Chem. Phys.* **1993**, *98*, 4195. Buch, V.; Silva, S. C.; Devlin, J. P. *J. Chem. Phys.* **1993**, *99*, 2265.
(17) Rowland, B.; Kadagathur, N. S.; Devlin, J. P. *J. Chem. Phys.* **1995**, *102*, 13. Buch, V.; Delzeit, L.; Blackledge, C.; Devlin, J. P. *J. Phys. Chem.* **1996**, *100*, 10076.
(18) Delzeit, L.; Devlin, M. S.; Rowland, B.; Devlin, J. P.; Buch, V. *J. Phys. Chem.* **1996**, *100*, 10076. Delzeit, L.; Devlin, J. P.; Buch, V. *J. Chem. Phys.* **1997**, *107*, 3726
(19) Delzeit, L.; Powell, K.; Uras, N.; Devlin, J. P. *J. Phys. Chem. B* **1997**, *101*, 2327.

(20) Uras, N.; Rahman, M.; Devlin, J. P. *J. Phys. Chem. B* **1998**, *102*, 9375. Devlin, J. P.; Uras, N.; Rahman, M.; Buch, V. *Isr. J. Chem.* **1999**, *39*, 261.

(21) Torchet, G.; Schwartz, P.; Farges, J., de Feraudy, M. F.; Raoult, B. *J. Chem. Phys.* **1983**, *79*, 6196.

(22) Bartell, L. S.; Huang, J. *J. Phys. Chem.* **1994**, *98*, 7455. Huang, J.; Bartell, L. S. *J. Phys. Chem.* **1995**, *99*, 3924.

(23) Devlin, J. P.; Joyce, C.; Buch, V. *J. Phys. Chem. A* **2000**, *104*, 1974.

(24) Buch, V.; Sandler, P.; Sadlej, J. *J. Phys. Chem. B* **1998**, *102*, 8641.

(25) Jorgensen, W. L.; Chandrasekhar, J.; Madura, J. D.; Impey, R. W.; Klein, M. L. *J. Chem. Phys.* **1983**, *79*, 926.

(26) Impey, R. W.; Klein, M. L. *Chem. Phys. Lett.* **1984**, *104*, 579.

(27) Rzepkowska, J. MSc. thesis, Warsaw University.

(28) Rzepkowska, J.; Uras, N.; Sadlej, J.; Buch, V. Manuscript in preparation.

(29) Kendall, A.; Dunning, T. H.; Harrison, R. J. *J. Chem. Phys.* **1992**, *96*, 6796.

(30) Boys, S. F.; Bernardi, F. *Mol. Phys.* **1970**, *19*, 553.

(31) (a) Sandler, P.; Jung, J.; Szczesniak, M. M.; Buch, V. *J. Chem. Phys.* **1994**, *101*, 1378. (b) Sandler, P.; Buch, V.; Sadlej, J. *J. Chem. Phys.* **1996**, *105*, 10387.

(32) Stockman, P. A.; Bumgarner, R. E.; Suzuki, S.; Blake, G. A. *J. Chem. Phys.* **1992**, *96*, 2496.

(33) In the simulation, the water HOH angle was readjusted from the one used in the ab initio study (105.52°) to 104.52°, to match TIP4P geometry; the readjustment caused minor changes in the PES.

(34) Goldstein, H. *Classical Mechanics*; Addison-Wesley: Reading, MA1980.

(35) Uras, N.; Devlin, J. P. *J. Phys. Chem. A* **2000**, *104*, 5770.

(36) Buch, V. *J. Chem. Phys.* **1992**, *96*, 3814.

(37) Rowland, B.; Kadagathur, S.; Devlin, J. P.; Buch, V.; Feldmann, T.; Wojcik, M. *J. Chem. Phys.* **1995**, *102*, 8328.

(38) (a) Olovsson, I.; Templeton, D. H. *Acta Crystallogr.* **1959**, *12*, 827. (b) Siemons, W. J.; Templeton, D. H. *Acta Crystallogr.* **1954**, *7*, 194. (c) Bertie, J. E. Devlin, J. P. *J. Chem. Phys.* **1984**, *81*, 1559. (d) Bertie, J. E.; Shehata, M. R. *J. Chem. Phys.* **1985**, *83*, 1449.